The dipolar endofullerene HF@C_{60}.

Andrea Krachmalnicoff,[†] Richard Bounds,[†] Salvatore Mamone,[‡] Shamim Alom,[†] Maria Concistrè,[†] Benno Meier,[†] Karel Kouřil,[†] Mark E. Light[†], Mark R. Johnson,[§] Stéphane Rols,[§] Anthony J. Horsewill,[‡] Anna Shugai, [⊥] Urmas Nagel, [⊥] Toomas Rõõm, [⊥] Marina Carravetta,[†] Malcolm H. Levitt,[†] and Richard J. Whitby*[†]

[†] Chemistry, University of Southampton, Southampton SO17 1BJ, United Kingdom.

[‡] School of Physics and Astronomy, University of Nottingham, Nottingham NG7 2RD, United Kingdom

[§] Institut Laue-Langevin, CS 20156, 38042 Grenoble, France

[⊥]National Institute of Chemical Physics and Biophysics, Akadeemia Tee 23, Tallinn 12618, Estonia

* rjw1@soton.ac.uk

Abstract: The cavity inside fullerenes provides a unique environment for the study of isolated atoms and molecules. We report encapsulation of hydrogen fluoride inside C_{60} using molecular surgery to give the endohedral fullerene HF@C_{60}. The key synthetic step is the closure of the open fullerene cage while minimizing escape of HF. The encapsulated HF molecule moves freely inside the cage and exhibits quantization of its translational and rotational degrees of freedom, as revealed by inelastic neutron scattering and infrared spectroscopy. The rotational and vibrational constants of the encapsulated HF molecules were found to be redshifted relative to free HF. The NMR spectra display a large ^{1}H-^{19}F J-coupling typical of an isolated species. The dipole moment of HF@C_{60} was estimated from the temperature-dependence of the dielectric constant at cryogenic temperatures and showed that the cage shields around 75% of the HF dipole.

Molecular endofullerenes consist of fullerene cages encapsulating small molecules, which are free to rotate and translate inside the cage.[1] The dihydrogen and water endofullerenes H_2@C_{60}, H_2O@C_{60}, and their isotopologues, have been synthesized by the procedure known as 'molecular surgery', in which synthetic operations are used to open a hole in the fullerene allowing encapsulation of the guest, followed by a suturing technique to reform the pristine fullerene shell.[2-4] Recently the approach has been extended to C_{70} and $C_{59}N$.[5-7] The confined molecules display quantization of their coupled translational and rotational degrees of freedom, and exhibit phenomena such as nuclear spin isomerism and ortho-para conversion.[8-12] Recently it was shown that nuclear spin conversion of the encapsulated water molecules in H_2O@C_{60} leads to a change in the dielectric constant of the material.[13]

One system of great interest is HF@C_{60}, in which each fullerene cage contains a single hydrogen fluoride (HF) molecule. This material offers the possibility to study the spectroscopic properties of near-isolated and freely rotating HF molecules under a wide range of conditions, free from the complications of dimerization and hydrogen bonding. Predictions of the properties of HF@C_{60} have been made using classical,[14] semiempirical[15,16] and quantum chemistry techniques.[17-20] Furthermore it has been postulated that endofullerenes containing freely rotating electric dipoles could exhibit ferroelectricity, due to cooperative alignment of the interacting electric dipole moments.[21]

The first examples of open–cage endofullerenes encapsulating a hydrogen fluoride molecule have recently appeared, including HF@**1**.[22,23] Herein we report the successful suturing of HF@**1** to give the closed-cage species HF@C_{60}. We present NMR, infrared, and neutron scattering data on HF@C_{60} which show that the translational and rotational motions of the HF molecule inside the cage are quantized. Interactions with the cage modify the rotational and vibrational constants of the encapsulated HF molecule. The fullerene cages strongly shield the electric dipole moments of the endohedral HF molecules.

Results and discussion

Attempting to close HF@**1** to give HF@**4** (Figure 1) by heating with triphenylphosphine (PPh_3), as previously described for H_2O@**1**[4] lead to complete loss of HF and isolation of empty **4**. The initial step in the reaction is dehydration to form the tetraketone **2**, normally occurring spontaneously under the high temperature conditions used. DFT calculations gave an activation energy of 74.9 kJ/mol for the exit of HF from the cavity of **2**; in comparison the calculated activation energy for the release of H_2O from the same cage was 115.0 kJ/mol (Supplementary Table 1). Stirring HF@**1** with 3Å molecular sieves at room temperature allowed formation of HF@**2** without significant loss of the endohedral molecule. HF@**2** reacted slowly with PPh_3 at room temperature to afford the unusual isolable phosphorous ylid HF@**3** (PR_3=PPh_3), again with retention of HF. However heating of HF@**3** to 110 °C was required to complete the intramolecular Wittig reaction causing loss of HF to give empty **4**. The regiochemistry of the ylid **3** was confirmed by a 9.6 Hz coupling between the phosphorous and the adjacent carbonyl carbon, and by good agreement of the calculated ^{13}C spectra of only the isomer shown with experimental values (Supplementary Figure 1). To accelerate the conversion of HF@**3** to HF@**4** we tried the electron deficient tri(2-furyl)phosphine (PFu_3)[24] instead of PPh_3. Although the ylid HF@**3** (PR_3 = PFu_3) was not observed indicating that the intramolecular Wittig reaction **3** to **4** had been accelerated, the initial reaction of phosphine with tetraketone HF@**2** required heating to 70 °C, and empty **4** was again formed.

A successful compromise was found with $PPh(Fu)_2$ which reacted with HF@**1** in the presence of molecular sieves at room temperature to give HF@**4** in 64% yield still containing 30% HF. The orifice of HF@**4** can be sutured as reported for H_2O@**4** without further loss of the endohedral molecule.[4] Thus 30% filled HF@C_{60} was isolated after reduction of HF@**4** with triisopropylphosphite to afford HF@**5** followed by reaction with N-phenylmaleimide (Figure 1). Overall sublimed 30% filled HF@C_{60} is produced in three steps and 36% yield from 50% filled HF@**1**. HPLC on a Buckyprep® column can be used to separate HF@C_{60} (retention time = 8.05 min) from C_{60} (retention time = 7.81 min) to afford a quantitatively filled sample.

A crystal structure of the carbon-disulfide solvate of HF@C_{60} was obtained (CCDC 1453465. Supplementary Figure 2) and is similar to that that reported for the equivalent C_{60} solvate[25] with the exception of a spherically symmetrical electron distribution in the centre of the fullerene corresponding to the HF molecule. Since the HF molecule is freely rotating in the cage at temperatures far below that used for the X-ray structure determination (100 K) we would not expect to observe either the hydrogen atom, or indeed a displacement of the fluorine from the centre of the cage. Both structures show slight distortion of the cages from spherical, probably due to crystal packing forces. For C_{60} the two crystallographically distinct molecules have long/short axis of 7.100(7)/7.033(7) and 7.100(6)/7.038(6) whereas for HF@C_{60} the corresponding ratios are 7.122(9)/7.039(9) and 7.107(9)/7.02(1). The slightly greater mean ratio for HF@C_{60} (1.012 cf 1.009) is not significant to 3σ so the effect of the endohedral molecule on the structure of the carbon cage is inconclusive. There have been similar observations for H_2O@C_{60}.[26] UV-spectra and electrochemical studies on HF@C_{60} were indistinguishable from the parent C_{60}[27] indicating that the endohedral molecule has no significant effect on the orbital energy levels of the cage (Supplementary Table 2, Figures 3 and 4).

The ^{1}H NMR spectrum of HF@C_{60} shows a doublet with $^1J_{HF}$ of 505.5 ± 0.5 Hz at δ_H = –2.68 ppm, the upfield shift being due to the shielding effect of the C_{60} cage. The large $^1J_{HF}$ value is the same as that reported for HF in open fullerenes,[22,23] is comparable to the 529 ± 23 Hz reported for HF in a molecular beam,[28] and is larger than the coupling constants reported for HF in a variety of solvents (410-479 Hz).[29] The ^{13}C NMR spectrum of HF@C_{60} shows a sharp singlet at δ = 142.85 ppm. The downfield shift of 0.05 ppm relative to empty C_{60} deviates from the empirical correlation drawn previously between the van der Waals radius of the endohedral guest and a downfield ^{13}C chemical shift ($H_2O@C_{60}$, 0.11 ppm; $H_2@C_{60}$, 0.08 ppm; He@C_{60} 0.02 ppm).[2,3,30]

A series of ^{19}F NMR spectra of HF@C_{60} in the polycrystalline solid state were acquired at 263 K, using magic-angle spinning at a range of rotation frequencies, without ^{1}H decoupling (Figure 2 and Supplementary Figures 5 and 6). All spectra display a prominent splitting due to a ^{1}H-^{19}F J-coupling of 506 ± 0.5 Hz. The magic-angle-spinning NMR spectra display small spinning sidebands, indicating the presence of anisotropic spin interactions. The similar sideband amplitudes for the two components of the J-split doublet indicate that the dominant anisotropic mechanism in this case is chemical shift anisotropy, probably associated with either a geometric or an electronic Jahn-Teller distortion of the encapsulating fullerene cage. Solid state ^{1}H and ^{13}C NMR spectra were also obtained (Supplementary Figures 7 and 8).

Inelastic neutron scattering (INS) and infrared (IR) absorption spectra were acquired on HF@C_{60} at low temperature (Figure 3). Far-IR and mid-IR spectra were recorded at 5 K, while the INS spectrum was recorded at 1.6 K using the incident neutron wavelength λ_n = 2.22 Å.

The endohedral HF molecule may be modeled as a vibrating rotor confined in the potential generated by C_{60}. The translational modes are defined by the motion of the center of mass of HF within its cage, resembling a three-dimensional quantum oscillator.[31,32] Therefore quantization of the vibrational, rotational and translational excitations is defined by the quantum numbers v = 0, 1.., J = 0, 1.., and N = 0, 1.., respectively.[33,34] An energy level diagram for the confined rotor is shown in Figure 3(c).

At sufficiently low temperatures all the observable transitions originate from the vibrational, translational and rotational ground state of the confined HF molecules. The spectra display rotational and translational transitions of HF inside its C_{60} cage. The peak at 33 cm^{-1} (4.1 meV, labelled #1) is assigned to HF rotation, namely the transition J=0→J=1. In the INS spectrum this peak has excess width (FWHM 1.3 meV) indicating the presence of unresolved fine structure with splittings below 1 meV. This fine structure is partially resolved in the IR spectra. The peak at 11.0 meV (labelled #3) is assigned to the J=0→J=2 rotational transition. This transition is forbidden for IR spectroscopy but is observable by INS. The same set of IR transitions appears in the mid-IR range as sidebands to the vibrational transition v=0→v=1, located at 3791.1 cm^{-1}.

The INS and IR peak at 78.6 cm^{-1} (9.75 meV, labelled #2) is tentatively assigned to the translational transition, N=0→N=1. Analogous translational peaks have been observed for $H_2@C_{60}$.[35] A more detailed analysis is in progress to confirm this assignment.

The J=0→J=1 rotational transitions (#1 and #5) exhibit partially resolved structure, indicating that the 3-fold degeneracy of the J=1 state is lifted. An indication of breaking of icosahedral (nearly spherical) symmetry also comes from the finite intensity of the fundamental HF vibration transition v = 0 → v = 1 which is forbidden for free HF. This may be attributed to a Jahn-Teller breaking of icosahedral symmetry for the potential experienced by the HF molecule. Analogous behavior has been reported for the $H_2O@C_{60}$ complex[9,36] which also possesses a permanent electric dipole moment. The spinning sidebands in the ^{19}F magic-angle-spinning NMR spectra (Figure 2) indicate a finite chemical shift anisotropy for the endohedral molecule, and also indicate that the pure icosahedral symmetry of C_{60} is broken in the HF@C_{60} complex in the solid state.

The energies of the rotational and vibrational transitions of HF@C_{60} are significantly redshifted with respect to those of HF in the gas phase (Table 1). The change in the fundamental vibrational transition (-170.5 cm^{-1}) is in excellent agreement with that calculated by Dolgonos (-174 cm^{-1}),[17] and contrary to

other calculations which predicted a small blue-shift.[19] A redshift (-98.8 cm^{-1}) was also observed for $H_2@C_{60}$.[31] The rotational redshifts are attributed to a coupling of translational and rotational modes inside the cavity, and to cage-host interactions, which cause the inertial moment of the HF molecule to acquire some of the effective mass of the cage. The vibrational red-shift is due to lengthening, of the bond of the enclosed diatomic molecule indicating an attractive interaction with the cage.

Finally $HF@C_{60}$ is a 'dipole in a cage' and a key point of interest is the extent to which the cage shields the dipole. The electric dipole moment of $HF@C_{60}$ was estimated by measurement of its temperature-dependent dielectric constant as we recently described for $H_2O@C_{60}$.[13] The capacitance of a set of three equivalent capacitors containing pellets of 45% filled $HF@C_{60}$, C_{60} and one empty were simultaneously measured in the range 5K to 290K (Supplementary Figure 9). The polarizabilities of C_{60} and $HF@C_{60}$ are derived from the dielectric constants using the Clausius-Mossotti law as described in the (Supplementary section 1.12). The difference in polarizability below 100 K is attributed to the orientational polarizability of $HF@C_{60}$ and analyzed with the CMIStark software package[41] using the gas phase rotational constant[37] and the electric dipole moment as a free parameter. Good agreement is found for a dipole moment of 0.45±0.05 Debye (Figure 4). There are deviations from this behavior at high temperature which are not currently understood (Supplementary Figure 9).

The obtained dipole moment is in good agreement with some theoretical estimates[17,18,20] and indicates that shielding by the fullerene cage reduces the dipole moment of $HF@C_{60}$ to about 25% of that for isolated HF.[42,43] Calculations and measurements on $H_2O@C_{60}$ give similar results.[13,26,44]

Conclusion

In summary we have synthesized the endohedral fullerene $HF@C_{60}$ and characterized it by solution and solid-state NMR spectroscopy, observing the large $^1J_{HF}$ coupling indicative of an isolated molecule. Electrochemical studies and UV-spectroscopy show that the endohedral molecule has no detectable effect on the electronic structure of the cage. An X-ray crystal structure showed the presence of the endohedral HF, but was inconclusive if it caused a distortion of the cage. Low-temperature neutron scattering and infrared measurements indicate the quantization of vibrational, rotational and translational modes for the endohedral HF molecule. The rotational and vibrational transitions are red-shifted for the endohedral molecule, with respect to the free HF molecule in the gas phase. Some transitions display splittings which indicate a breaking of icosahedral symmetry, probably due to Jahn-Teller distortion. The X-ray structure also provides evidence for the breaking of symmetry. The electric dipole moment of $HF@C_{60}$ is only about 25% of that for isolated HF, showing that the cage has a strong shielding effect. Research is under way to characterize the potential energy surface of the endohedral molecule, to confirm the origin of the broken symmetry, and to further examine the electrical properties of the material.

Methods

Synthesis of HF@4: Activated 3Å molecular sieves (~4 g) were placed inside a Schlenk tube fitted with a J. Young tap. The tube was heated at 220 °C under vacuum (1 mmHg) for 1 hour before cooling to room temperature under nitrogen. Compound HF@**1** (50% filling factor, 520 mg, 0.456 mmol)[22] and di(furan-2-yl)(phenyl)phosphine[45] (1.930 g, 7.97 mmol) were added under a nitrogen flow followed by distilled oxygen free toluene (53 ml). The tube was sealed and stirred at room temperature in the dark. After 138 hours the reaction mixture was filtered and concentrated under reduced pressure. The crude product was purified by flash column chromatography over silica gel (eluent gradient: 1:1 toluene/hexanes to toluene). The fractions containing the spot running at R_f 0.5 (eluent: toluene) were collected and evaporated to dryness to afford compound HF@**4** as a black solid (30% filling factor, 324 mg, 64%).

Synthesis and characterisation data for HF@**3** (R = Ph), **3** (R = Ph), HF@**4**, HF@**5** and $HF@C_{60}$ (including HPLC purification and sublimation) are in the Supplementary sections 1.1-1.6.

DFT calculations. Calculations were carried out using the Gaussian 09 software package[46] using the B3LYP functional[47-49] and 6-31G(d) basis set.[50] For the exit of H_2O and HF from **2** a model for the fullerenes where the 6-tert-butylpyridyl groups were replaced by methyl groups was used. Grimme's D3 empirical dispersion correction using Becke - Johnson damping[51] was applied and energies were corrected for basis set superposition errors using the counterpoise method[52] and for zero point energies. Calculations of carbon-13 spectra for possible isomers of **3** were carried out by the Gauge-Independent Atomic Orbital (GIAO) method[53] using B3LYP and 6-311G(2d, p) basis set on full structures minimised at the B3LYP/6-31G(d) level.

Solid State NMR. Solid state ^{1}H, ^{13}C and ^{19}F NMR experiments were performed at 19.96 T (850 MHz) on a Bruker AVANCE III console at 263 K using magic angle spinning at 10 kHz, to increase resolution (or various spinning speeds to characterise anisotropic interactions).

Inelastic Neutron Scatering. The INS measurements were conducted at the Institut Laue-Langevin, Grenoble, using the IN4C time-of-flight spectrometer.[54] Two sample configurations were employed; a) a 3 mg sample of HF@C_{60} with 100% of fullerene cages filled with HF, b) a sample comprising 13 mg of 80% filled cages, plus 5 mg of 90% filled cages and 3 mg of 100% filled cages. Each sample was loaded inside an individual Al foil wrapper.

Infra Red. IR spectra were acquired on a pressed (60 MPa pressure) pellet (3 mm x 0.22 ± 0.01 mm) of polycrystalline 30% filled HF@C_{60} at 5K in a vacuum-tight sample chamber filled with He gas to a few mbar. The transmission spectra were measured with interferometer Vertex 80v (Bruker Optics) and two detectors were used: InSb detector (mid-IR range) and 4K bolometer (far-IR range).

Dielectric Constant. The dielectric constant measurements were preformed using the apparatus described previously.[13] Three capacitors are obtained by sandwiching the sample between two printed circuit boards (PCBs), each supporting three electrodes. Two fullerene pellets, comprising 30 mg of pure C_{60} and 31 mg HF@C_{60} (45% filled), respectively, were pressed in such a capacitance cell by applying a weight of 4 tons to the upper printed circuit board. Subsequently, the electrode distances of the C_{60}, HF@C_{60}, and empty capacitors were measured as 204±10, 274±10 and 192±10 μm respectively. The cell was mounted in a flow cryostat (typical He pressure 200 mbar). The capacitances of the two filled capacitors and an empty reference capacitor were measured at 16 kHz using two dual-channel Analog Devices AD7746 capacitance bridges, each interfaced to an Arduino Microcontroller. The temperature was measured using a Cernox sensor attached to one of the PCBs.

References

1. Levitt, M. H. Spectroscopy of light-molecule endofullerenes. *Phil. Trans. Royal Soc. A* **371**, 20120429 (2013).
2. Murata, M., Murata, Y. & Komatsu, K. Synthesis and properties of endohedral C_{60} encapsulating molecular hydrogen. *J. Am. Chem. Soc.* **128**, 8024 – 8033 (2006).
3. Kurotobi, K. & Murata, Y. A single molecule of water encapsulated in fullerene C_{60}. *Science* **333**, 613 - 616 (2011).
4. Krachmalnicoff, A., Levitt, M. H. & Whitby, R. J. An optimised scalable synthesis of $H_2O@C_{60}$ and a new synthesis of $H_2@C_{60}$. *Chem. Commun.* **50**, 13037 - 13040 (2014).
5. Murata, M., Maeda, S., Morinaka, Y., Murata, Y. & Komatsu, K. Synthesis and reaction of fullerene C_{70} encapsulating two molecules of H_2. *J. Am. Chem. Soc.* **130**, 15800 – 15801 (2008).
6. Hashikawa, Y., Murata, M., Wakamiya, A. & Murata, Y. Synthesis and Properties of Endohedral Aza[60]fullerenes: $H_2O@C_{59}N$ and $H_2@C_{59}N$ as Their Dimers and Monomers. *J. Am. Chem. Soc.* **138**, 4096 – 4104 (2016)
7. Zhang, R. *et al*. Synthesis of a distinct water dimer inside fullerene C_{70}. *Nature Chem.* 8, 435 – 441 (2016).

8. Levitt, M. H. & Horsewill, A. J. Nanolaboratories: physics and chemistry of small-molecule endofullerenes. *Phil. Trans. Royal Soc. A* **371**, 20130124 (2013).
9. Beduz, C. *et al*. Quantum rotation of *ortho* and *para*-water encapsulated in a fullerene cage. *Proc. Nat. Acad. Sc.* **109**, 12894 - 12898 (2012).
10. Lopez-Gejo, J. *et al*. Can H_2 inside C_{60} communicate with the outside world? *J. Am. Chem. Soc.* **129**, 14554 - 14555 (2007).
11. Mamone, S. *et al*. Nuclear spin conversion of water inside fullerene cages detected by low-temperature nuclear magnetic resonance. *J. Chem. Phys.* **140**, 194306 (2014).
12. Mamone, S. *et al*. Rotor in a cage: Infrared spectroscopy of an endohedral hydrogen-fullerene complex. *J. Chem. Phys.* **130**, 081103 (2009).
13. Meier, B. *et al*. Electrical detection of ortho–para conversion in fullerene-encapsulated water. *Nature Commun.* **6**, 8112 (2015).
14. Varandas, A. J. C. A simple model for vibrational stretching in diatomics at fullerenes. *Asian J. Spectroscopy* **3**, 79-90 (1999).
15. Williams, C. I., Whitehead, M. A. & Pang, L. Interaction and dynamics of endohedral gas molecules in C_{60} isomers and C_{70}. *J. Phys. Chem.* **97**, 11652 – 11656 (1993)
16. Hernández-Rojas, J., Bretón, J. & Gomez Llorente, J. M. A semi-empirical analytical potential for diatomic molecules at spherical fullerenes. *Chem. Phys. Lett.* **222**, 88-94 (1994).
17. Dolgonos, G. A. & Peslherbe, G. H. Encapsulation of diatomic molecules in fullerene C_{60}: implications for their main properties. *Phys. Chem. Chem. Phys.* **16**, 26294 - 26305 (2014).
18. Cioslowski, J. Endohedral chemistry: Electronic structures of molecules trapped inside the C_{60} cage. *J. Am. Chem. Soc.* **113**, 4139 - 4141 (1991).
19. Shameema, O., Ramachandran, C. N. & Sathyamurthy, N. Blue shift in X-H stretching frequency of molecules due to confinement. *J. Phys. Chem. A.* **110**, 2 - 4 (2006).
20. Galano, A., Pérez-González, A., del Olmo, L., Francisco-Marquez, M. & León-Carmona, J. R. On the chemical behavior of C_{60} hosting H_2O and other isoelectronic neutral molecules. *J Mol. Mod.* **20**, 2412 (2014).
21. Cioslowski, J. & Nanayakkara, A. Endohedral fullerites: A new class of ferroelectric materials. *Phys. Rev. Lett.* **69**, 2871 - 2873 (1992).
22. Krachmalnicoff, A. *et al*. Synthesis and characterisation of an open-cage fullerene encapsulating hydrogen fluoride. *Chem. Commun.* **51**, 4993 - 4996 (2015).
23. Xu, L. *et al*. Release of the water molecule encapsulated inside an open-cage fullerene through hydrogen bonding mediated by hydrogen fluoride. *Chem. Eur. J.* **21**, 13539 – 13543 (2015).
24. Appel, M., Blaurock, S. & Berger, S. A. Wittig reaction with 2-furyl substituents at the phosphorus atom: Improved (Z) selectivity and isolation of a stable oxaphosphetane intermediate. *Eur. J. Org. Chem.* 1143 - 1148 (2002).
25. Olmstead, M. M., Jiang, F. & Balch, A. L. $2C_{60}{\cdot}3CS_2$: Orientational ordering accompanies the reversible phase transition at 168 K. *Chem. Commun.* 483 – 484 (2000).
26 Aoyagi, S. *et al*. A cubic dipole lattice of water molecules trapped inside carbon cages. *Chem. Commun.* **50**, 524 – 526 (2014).
27. Xie, Q., Pérez-Cordero, E. & Echegoyen, L. Electrochemical detection of C_{60}^{6-} and C_{70}^{6-}: Enhanced stability of fullerides in solution. *J. Am. Chem. Soc.* **114**, 3978-3980 (1992).
28. Muenter, J. S. Hyperfine structure constants of HF and DF. *J. Chem. Phys.* **52**, 6033 - 6037(1970).
29. Martin, J. S. & Fujiwara, F. Y. High resolution nuclear magnetic resonance spectra of hydrogen fluoride in solution and in bihalide ions. Nuclear spin coupling in strong hydrogen bonds. *J. Am. Chem. Soc.* **96**, 7632 - 7637 (1974).
30. Morinaka, Y., Tanabe, F., Murata, M., Murata, Y. & Komatsu, K. Rational synthesis, enrichment, and ^{13}C NMR spectra of endohedral C_{60} and C_{70} encapsulating a helium atom. *Chem. Commun.* **46**, 4532 (2010).

31. Ge, M., *et al*. Interaction potential and infrared absorption of endohedral H_2 in C_{60}. *J. Chem. Phys.* **134**, 054507 (2011).
32. Ge, M. *et al*. Infrared spectroscopy of endohedral HD and D_2 in C_{60}. *J. Chem. Phys.* **135**, 114511 (2011).
33. Cohen-Tannoudji, C., Diu, B. & Laloe, F. *Quantum Mechanics, vol. 1*, 1 edition ed., Wiley VCH, 1977.
34. Flügge, S. *Practical Quantum Mechanics*, Springer, 1998.
35. Horsewill, A. J. *et al*. Quantum rotation and translation of hydrogen molecules encapsulated inside C_{60}: temperature dependence of inelastic neutron scattering spectra. *Phil. Trans. Royal Soc. A* **371**, 20110627 (2013).
36. Goh, K. K. S. *et al*. Symmetry-breaking in the endofullerene $H_2O@C_{60}$ revealed in the quantum dynamics of ortho and para-water: a neutron scattering investigation. *Phys. Chem. Chem. Phys.* **16**, 21330 - 21339 (2014).
37. Jennings, D. A. *et al*. High-resolution spectroscopy of HF from 40 to 1100 cm^{-1}: Highly accurate rotational constants. *J. Mol. Spectrosc.* **122**, 477 - 480 (1987).
38. Le Duff, Y. & Holzer, W. Raman scattering of HF in the gas state and in liquid solution. *J. Chem. Phys.* **60**, 2175 – 2178 (1974).
39. Kuipers, G. A., Smith, D. F. & Nielsen, A. H. Infrared spectrum of hydrogen fluoride. *J. Chem. Phys.* **25**, 275 - 279 (1956).
40. Atkins, P. & de Paula, J. *Atkins' Physical Chemistry* (Oxford University Press, 2010).
41. Chang, Y. P., Filsinger, F., Sartakov, B. G. & Küpper, J. CMIstark: Python package for the Stark-effect calculation and symmetry classification of linear, symmetric and asymmetric top wavefunctions in dc electric fields. *Comput. Phys. Commun.* **185**, 339–349 (2014).
42. Delaney, P. & Greer, J. C. C_{60} as a Faraday cage. *Appl. Phys. Lett.* **84**, 431-433 (2004).
43. Cioslowski, J. & Fleischmann, E. D. Endohedral complexes: Atoms and ions inside the C_{60} cage. *J. Chem. Phys.* **94**, 3730–3734 (1991).
44. Ensing, B.; Costanzo, F. & Silvestrelli, P. L. On the polarity of buckminsterfullerene with a water molecule inside. *J. Phys. Chem. A* **116**, 12184 – 12188 (2012).
45. Märkl, G., Amrhein, J., Stoiber, T., Striebl, U. & Kreitmeier, P. 5,16-Dialkyl(diaryl)-5,16-dihydro-5,16-diphospha- tetraepoxy[22]annulene(2.1.2.1). *Tetrahedron* **13**, 2551 – 2567 (2002)
46. Frisch, M. J. *et al*. Gaussian 09, Rev D.01, Gaussian, Inc., Wallingford CT, (2009).
47. Becke, A. D. Density-functional thermochemistry. III. The role of exact exchange. *J. Chem. Phys.* **98**, 5648 - 5652 (1993).
48. Lee, C., Yang, W. & Parr, R. G. Development of the Colic-Salvetti correlation-energy formula into a functional of the electron density. *Phys. Rev. B* **37**, 785-789 (1988)
49. Stephens, P. J., Devlin, F. J., Chabalowski, C. F. & Frisch, M. J. *Ab initio* calculation of vibrational absorption and circular dichroism spectra using density functional force fields. *J. Phys. Chem.* **98**, 11623 (1994).
50. Hehre, W. J., Radom, L., Schleyer P. v. R. & Pople, J. A. *Ab initio molecular orbital theory*, (John Wiley & Sons, New York, 1986).
51. Grimme, S., Ehrlich, S. & Goerigk, L. Effect of the damping function in dispersion corrected density functional theory. *J. Comput. Chem.* **32**, 1456 – 1465 (2011).
52. Boys, S. F. & Bernardi, F. The calculation of small molecular interactions by the differences of separate total energies. Some procedures with reduced errors. *Mol. Phys.* **19**, 553-556 (1970).
53. Cheeseman, J. R., Trucks, G. W., Keith, T. A. & Frisch, M. J. A comparison of models for calculating nuclear magnetic resonance shielding tensors. *J. Chem. Phys.* **104**, 5497-5509 (1996).
54. http://www.ill.eu/fileadmin/users_files/Other_Sites/YellowBook2008CDRom/ index.htm

Acknowledgments

This research was supported by the EPSRC (UK) (EP/1029451, M001962, M001970) including core capability (EP/K039466) and the European Regional Development Fund Interreg-IVB, MEET project. MC thanks the Royal Society for a University Research Fellowship. We are grateful to the UK 850 MHz solid-state NMR Facility at Warwick. The research in Tallinn was sponsored by the Estonian Ministry of Education and Research grant IUT23-3 and the European Regional Development Fund project TK134.

Author contributions

The project was conceived by RJW with the research and analysis coordinated by RJW, MHL, AJH, MCa and TR. The manuscript was written by RJW, AK, MHL, AJH, SM, RB, TR and MCo. RJW conceived and AK and SA carried out the synthesis and basic characterization (solution NMR, electrochemistry, UV, MS, HPLC); The solid state NMR was coordinated by MCa and carried out by RB with assistance from MCo for the analysis; TR coordinated and AS and UN carried out the IR measurements; AJH coordinated, and AJH, SM, MRJ and SR carried out the INS experiments. SM, TR and AJH analyzed the INS and IR measurements with modeling of the quantum dynamics of the confined HF carried out by SM, AJH, TR and MHL. BM coordinated and BM, KK, and SA carried out the dielectric constant measurements. The crystal structure was acquired and solved by ML.

Additional information

Supplementary information and chemical compound information are available in the online version of the paper. Reprints and permissions information is available online at www.nature.com/reprints. Correspondence and requests for materials or original research data should be addressed to RJW.

Competing financial interests

The authors declare no competing financial interests.

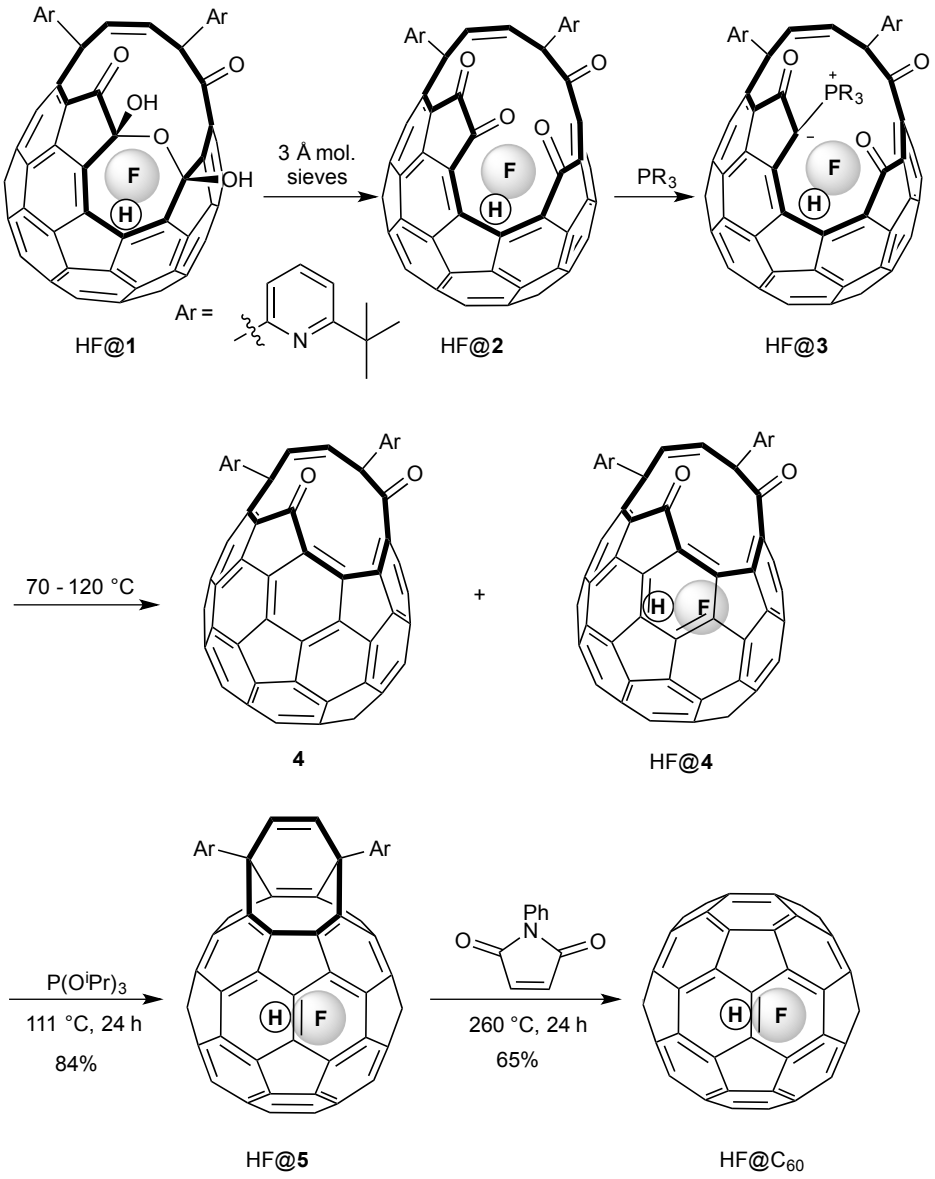

Figure 1. Synthesis of HF@C_{60} from HF@**1**. With PPh_3 loss of HF from HF@**3** was faster than the elimination of PPh_3O giving empty **4**; with P(2-furyl)$_3$ the formation of **3** required a higher temperature and HF was again lost; with PPh(2-furyl)$_2$ the endohedral HF survived both stages giving HF@**4**.

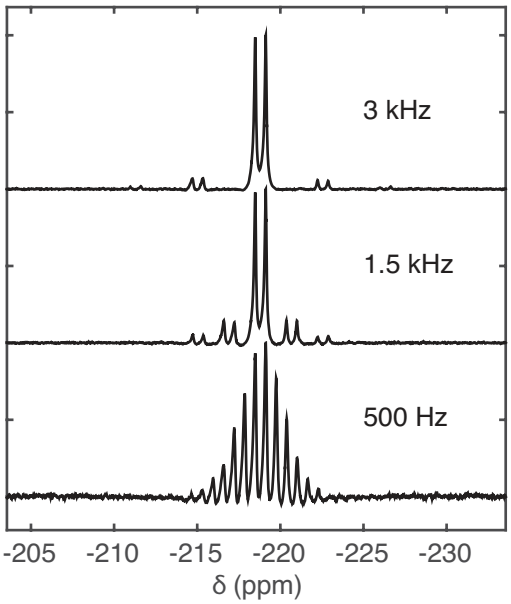

Figure 2. ^{19}F NMR spectra of HF@C_{60} in the polycrystalline solid state at three different magic-angle-spinning frequencies. The top spectrum displays a clear doublet structure due to the ^{1}H-^{19}F J-coupling, with two sets of spinning sidebands on either side, caused by a chemical shift anisotropy interaction induced by an electronic or structural distortion of the enclosing fullerene cage. The spinning sidebands shift closer to the main peaks and increase in amplitude as the spinning frequency is decreased (lower two panes). All data were obtained at a magnetic field of 19.96 T and sample temperature of 263 K.

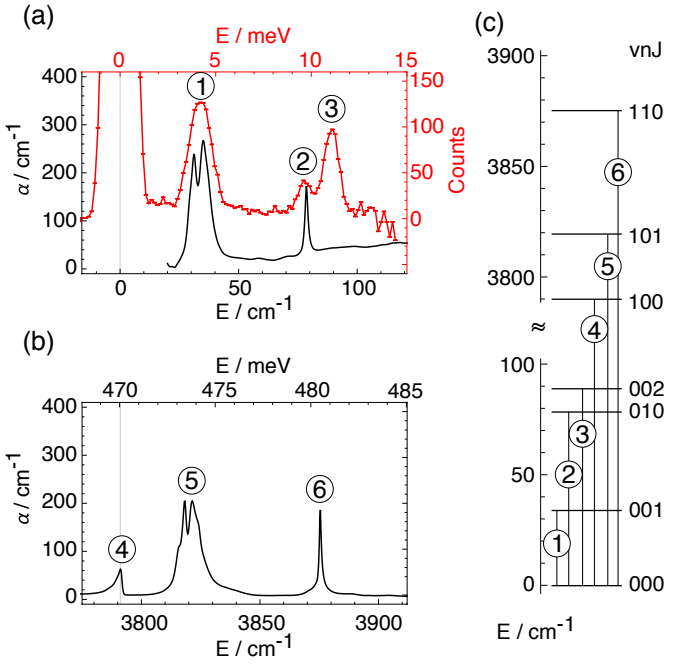

Figure 3. Energy levels of confined HF. (a) INS at 1.6 K (red) and far-IR spectra at 5 K (black) of polycrystalline HF@C_{60}. (b) Mid-IR spectrum of HF@C_{60} at 5 K. The figures have the same energy width across the horizontal scale and (b) is aligned so that the fundamental vibrational transition at 3791.1 cm^{-1} falls in line with the zero energy position in (a). (c) Energy levels and the assignments of the transitions using the vibrational (v), translational (N) and rotational (J) quantum numbers.

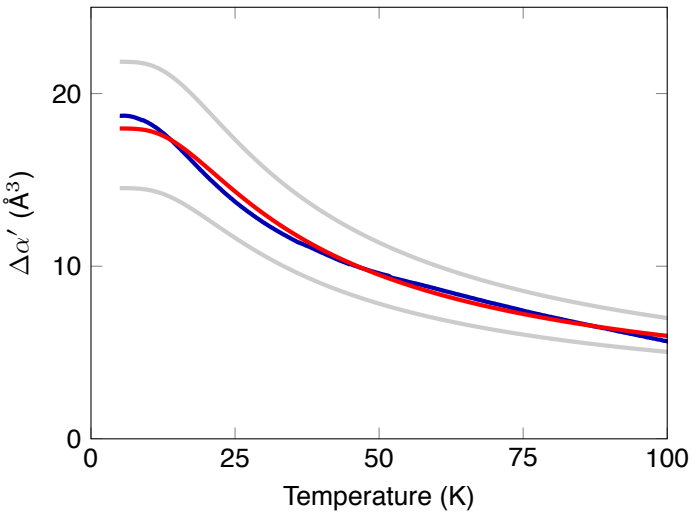

Figure 4. Estimate of the electric dipole moment based on the temperature dependence of the bulk dielectric constant. The blue line shows the difference in molecular polarizability volumes of HF@C_{60} and C_{60}, estimated from dielectric constant measurements. The data are well represented by a linear rotor with the HF gas phase rotational constant, but a reduced dipole moment of 0.45 Debye (red curve). For comparison, the lower and upper gray curves show the expected polarizability for dipole moments of 0.4 and 0.5 Debye, respectively.

Table 1. Positions of the maxima for the observed transitions in HF@C_{60} and corresponding line positions of free HF.[a]

Trans.	vNJ→v'N'J'	HF@C_{60}	HF gas
1	000→001	31.1, 35.0	41.11 (ref 37)
2	000→010	78.6	n.a.
3	000→002	88.72	122.5 (ref 38)
4	000→100	3791.1	3961.64 (ref 38)
5	000→101	3818.4, 3821.5	4001.27 (ref 39)
6	000→110	3875.5	n.a.

[a] For HF@C_{60} the states are defined by vNJ quantum numbers, and for HF in the gas phase by vJ only. All transitions are in cm^{-1} units.